ISSN: 2345-3109

RCEE
Research in Civil and Environmental Engineering

www.jrcee.com
Research in Civil and Environmental Engineering 2014 2 (03) 96-119

PUSHOVER ANALYSIS OF UNREINFORCED MASONRY STRUCTURES BY FIBER FINITE ELEMENT METHOD

A. H. Akhaveissy [a*], M. Abbassi [b]

[a] Department of Civil Engineering, Faculty Engineering, Razi University, Kermanshah, Iran.

[b] Department of Civil Engineering, Faculty Engineering, University of Kurdistan, Sanandaj, Iran

Keywords

Masonry wall

Macro-modeling

Fiber model

2D pushover analyses

Finite element analysis

A B S T R A C T

A 2D finite element analysis for the numerical prediction of capacity curve of unreinforced masonry (URM) walls is conducted. The studied model is based on the fiber finite element approach. The emphasis of this paper will be on the errors obtained from fiber finite element analysis of URM structures under pushover analysis. The masonry material is modeled by different constitutive stress-strain model in compression and tension. OpenSees software is employed to analysis the URM walls. Comparison of numerical predictions with experimental data, it is shown that the fiber model employed in OpenSees cannot properly predict the behavior of URM walls with balance between accuracy and low computational efforts. Additionally, the finite element analyses results show appropriate predictions of some experimental data when the real tensile strength of masonry material is changed. Hence, from the viewpoint of this result, it is concluded that obtained results from fiber finite element analyses employed in OpenSees are unreliable because the exact behavior of masonry material is different from the adopted masonry material models used in modeling process.

1 INTRODUCTION

Masonry is among the oldest material which is used for constructing the buildings and has been considered as the most durable. Masonry is a composite material which consists of units and mortar joints. Prominent new developments in masonry materials and applications have happened in the past two decades. Nowadays, there are a great number of masonry structures around the world. Therefore, the analysis of masonry structures is in considerable interest in various areas of structural and earthquake engineering. Due to its geometrical characteristics, these structures maybe idealized as frames. Masonry buildings are constructed in many parts of the world where earthquakes occur. It has been observed in major recent earthquakes that masonry buildings experienced more serious damages than did concrete

[*]Corresponding author (Phone: + *98 (831) 4274535*; Fax: + *98 (831) 4274542*; E-mail: *Ahakhaveissy@razi.ac.ir*).

buildings such as in 1990 Manjil (Moghaddam, 2006), 1971 San Fernando and 1994 Northridge earthquakes (Bruneau, 1995). If a realistic nonlinear analysis of a masonry structures be carried out, the safety of the structure is increased and the cost can frequently be reduced. Hence, the knowledge of their seismic behavior is necessary so as to evaluate the seismic performance of masonry structures. Because of high computational costs required to perform nonlinear dynamic time-history analysis, the pushover analysis, is a very attractive method to estimate the seismic response of structures due to its simplicity and efficiency (Jingjiang et al., 2003; Makarios, 2005; Jiang et al., 2010). Pushover analysis is commonly used to estimate the real displacements and forces developed in the members due to ground motion in the structures. Therefore, pushover analysis is used in order to determine the capacity curve of URM walls in this presented paper.

After major earthquakes occurred in the past three decades (1987 Whittier, 1989 Loma Prieta, 1990 Manjil and 2003 Bam) the necessity for using ever more accurate methods for evaluating seismic demand on masonry structures became evident. Nowadays the finite element method is the most general and one of the most powerful tools for the analysis of masonry structures. For the design of new structures or capacity assessment of existing ones, nonlinear analyses allows for a better representation of the structural response under any loading conditions, and under earthquake loading in particular (Rodrigues et al., 2012). During recent year, interest in the nonlinear analysis of masonry structures has increased stably, because of the wide use of masonry as a structural material, in the form of reinforced and unreinforced masonry walls and due to the development of relatively powerful nonlinear analysis techniques implemented on electronic digital computers. It is natural that with the development of the finite element method a large number of different finite elements models have been formulated for the analysis of masonry structures. Two methodologies exist for modeling the behavior of masonry structures including: macro and micro-element modeling. An approach for analysis of unreinforced masonry buildings that is very used is the macro-modeling of masonry as a composite material. The macro-modeling is more practice oriented due to the reduce time and memory requirements as well as a user-friendly mesh generation. In the field of numerical approach, various authors have proposed the finite element models for predicting the response of URM buildings under different loading conditions.

Milani et al. (2006) proposed a micro-mechanical model for the homogenized limit analysis of in-plane loaded masonry. The model assumes fully equilibrated stress fields in the elementary cell. The accuracy of the model has been assessed through meaningful comparisons both with kinematic approaches. A kinematic FE limit analysis for the 3D analysis of full masonry buildings subjected to horizontal actions to determine the ultimate lateral load was performed by Milani et al. (2007). To evaluating of the total internal power dissipated both in- and out-of-plane failures were taken into account. Linearized homogenized surfaces for masonry in six dimensions (Milani et al., 2006; Cecchi and Milani, 2008) were obtained and implemented in a finite element code. Comparisons between the predicted results from the 3D homogenized limit analysis and experimental data show an error of approximately 12%.

Pasticier et al. (2008) conducted the seismic analyses of masonry buildings. To modeling the two unreinforced stone-masonry walls in the Catania Project, SAP2000 v.10 was used. Comparisons of numerical predictions obtained using nonlinear analysis by SAP2000 and results of the Basilicata research group have demonstrated the capability of the proposed model in providing close predictions of ultimate base shear forces. However, different results from SAP2000 and the SAM code, which was developed by the University of Pavia, were estimated.

Cecchi and Milani (2008) derived the macroscopic failure surfaces of two-wythes masonry arranged in English bond texture by using a Reissner–Mindlin kinematic limit analysis approach. The assumptions were that flow rule is associated both for the constituent materials and a finite subclass of possible deformation modes. The comparison between a 2D FE Reissner–Mindlin limit analysis approach and a full 3D heterogeneous FE model in terms of deformed shapes at collapse and failure loads shows the reliability of the results obtained using the kinematic identification approach proposed.

Park et al. (2009) studied seismic fragility of an unreinforced masonry of low-rise building. The used structural modeling method utilizes a simple, composite nonlinear spring. To modeling, the unreinforced masonry wall is divided into distinct areas or segments that are represented by a nonlinear spring. Additionally, the springs are assembled in series and in parallel to match the segment topology of the wall. Rota et al. (2010) focused on presenting a new analytical approach for the derivation of fragility curves of masonry buildings. The methodology was based on nonlinear stochastic analyses of building prototypes. In order to generating input variables from the probability density functions of mechanical parameters, Monte Carlo simulations were used.

Milani (2011) presented a simple homogenized model for the nonlinear and limit analysis of masonry walls in-plane loaded. The assumptions were that nonlinearity is concentrated on brick-brick interfaces and joints reduced to interface. Behavior of homogenized masonry was implemented at a structural level in a novel FE nonlinear code relying on an assemblage of rigid infinitely resistant triangular elements and nonlinear interfaces. Nonlinear analyses were conducted over laboratory test data.

Akhaveissy (2011) presented a new close form solution to determine the shear strength of unreinforced masonry walls. Predicted results show less error percentage than do ATC and FEMA-307 (1999). To modeling the mechanical response of mortar joints in masonry walls, the numerical implementation of a new proposed interface model was used. The theoretical framework was derived from plasticity theory. Consequently, the proposed closed form solution can be used satisfactorily to analyze unreinforced masonry structures.

Akhaveissy and Desai (2011) presented a unified model to characterize the behavior of masonry structures based on Disturbed State Concept (DSC) with modified hierarchical single yield surface (HISS) plasticity. The model was used by two HISS yield surfaces for compressive and tensile behavior. The comparisons of proposed constitutive model with results from test data showed proper accuracy. Additionally, a new explicit formula was also presented to estimate the strength of URM structures.

By utilizing accurate 3D Finite Element discretization, Milani et al. (2012) evaluated the seismic behavior of the Maniace Castle in Siracusa, Italy that was subjected to horizontal loads. The behavior of structure was analyzed in detail by means of different approaches. Comparison with a model representing the castle in its original configuration was provided.

Roca et al. (2012) presented a continuum model for the simulation of the viscous effects and the long-term damage accumulation in masonry structures. The rheological model was based on a generalized Maxwell chain representation, with a constitutive law utilizing a limited number of internal variables. The FE simulation of the construction process of the representative bay of Mallorca Cathedral was finally discussed, together with the analysis of the long-term effects.

Akhaveissy (2012a) presented a nonlinear finite element method with eight-nodded isoparametric quadrilateral elements to predict the behavior of unreinforced masonry structures in-plane loaded. The disturbed state concept (DSC) with modified hierarchical single yield surface (HISS) plasticity was used to characterize the constitutive behavior of masonry in both compression and tension. The DSC model allows for the characterization of non-associative behavior through the use of disturbance. The micro-cracking during deformation was computed, which eventually led to fracture and failure. The model was verified on laboratory specimens and real scale panels.

Akhaveissy (2012b) presented a simple efficient algorithm based on diagonal strength of URM walls to determine capacity curve of URM buildings. The Von Mises criterion was used to simulate the behavior of the units. Different masonry structures, including low- and high-rise masonry buildings, were analyzed using the presented algorithm. A comparison of results from the present work with experimental data and previous works showed proper accuracy from the present work.

Akhaveissy and Milani (2013a) proposed a simple, fully 2D macroscopic FE model for the seismic performance of real scale masonry structures in-plane loaded. To characterizing the constitutive behavior of masonry material the so called disturbed state concept (DSC) with modified hierarchical single yield surface (HISS) plasticity model with associated flow rules were used. It was experienced that a substantial reduction of the computational cost connected to the utilization of the DSC/HISS-CT model is obtained, especially in comparison with full smeared crack 3D approach available in the most diffused commercial codes. A new formula to estimate the ultimate lateral force of unreinforced masonry structures by Akhaveissy (2013) was presented. To modeling the mechanical response of mortar joints in masonry walls, an interface model was numerically implemented. The interface law was formulated in the elasto-plasticity framework for nonstandard materials with softening in the mortar joints. The theoretical framework of this study was based on the plasticity theory. The eight-nodded isoparametric quadrilateral elements and six-nodded contact elements is used in the finite element formulation. The comparisons of the loads that were predicted by proposed model with FEMA showed a lower error percentage than the FEMA guidelines. Akhaveissy and Milani (2013b) delivered a macro-model for the analysis of masonry shear walls reinforced with steel bar grids. The so-called Disturbed State Concept (DSC), with a modified hierarchical single yield surface (HISS-CT) plasticity model were used in order to simulate a distinct behavior in tension and compression of masonry material. Optimal reinforcement ratios were evaluated by means of the numerical model proposed. Good predictions of collapse loads were obtained overall ductility when compared to experimental data.

As illustrated, several models have been developed in the past two decades including macro and micro element modeling. The research results discussed related to macro-modeling processes showed considerable differences between different methods of macro-modeling in comparison with test data (Pasticier et al., 2008; Akhaveissy, 2012b). Moreover, the use of those models to predict the response of masonry buildings in common professional practice is not completely extended, because of difficulty of the theoretical background for practical engineers or the complexity of the material models involved. Therefore, the proposal of new models simplifying and reducing the computational effort with proper accuracy of the whole process of nonlinear analysis of masonry walls is of great importance. However, the extensive use of these models requires first a clear demonstration of its accuracy and reliability. Therefore, in this investigation, a fiber model is discussed to allow implementation in a macro-element approach using two-nodded nonlinear beam-column elements in a finite element framework by using OpenSees software.

To modeling the behavior of masonry material, the response of masonry is divided in two regions included: compression and tension. In compression region, the Hognestad model is used. For modeling the tension behavior, two constitutive material models is considered included elastic-perfectly plastic material and the model based on softening behavior which has obtained from the elastic behavior of masonry in the tensile region up to the peak tensile stress; softening behavior occurs after this point. Finally, for evaluating the performance of the proposed fiber element model, comparisons of finite element analyses results and available test data is presented.

2 FIBER MODEL ASSUMPTIONS-ELEMENT TYPE AND MODELING STRATEGY

Basically, finite element analyses involve three steps: the selection of a characteristic finite element model, the analysis of the model and the interpretation of the results, although in engineering practice the selection of an appropriate finite element model and the corresponding interpretation of the results are crucial, but a reliable and accurate response prediction with low computational cost and effort of the model is essential in order that the analysis results can be used with confidence (Bathe and Cimento, 1980). In this context, the fiber-element model provides a versatile approach to model the response of structural members. This model has shown that has a good response to predict the behavior especially for RC and steel structures including RC-columns, RC-beams, RC-frames, steel-beams, steel frames and bridge members under monotonic and earthquake loadings (Aschheim et al., 2007; Asgarian et al., 2010; Melo et al., 2011; Hashemi and Vaghefi, 2011; Adeli et al., 2011; Shamsaia et al., 2007; Lee and Mosalam, 2004; Hamutcuoglu and Scott, 2009; Shao et al., 2005). To modeling the behavior of unreinforced masonry walls considered in this study, fiber modeling strategy is used. In order to modeling by the fiber finite element methodology, URM walls is discretized both longitudinally into segments represented by discrete cross sections of the studied URM walls and at the cross section level, discretized into regions which are called fibers. The cross section response of the URM walls is derived by integration of the constitutive stress-strain behavior of the fibers. Consequently, Eq. (1) is used to compute the section resisting forces by summation of the axial force and bending moment contribution of all the fibers (Akhaveissy et al., 2013; Taucer et al., 1991).

$$D(x)=\begin{Bmatrix} M_y(x) \\ N(x) \end{Bmatrix}=\begin{Bmatrix} \sum_{ifib=1}^{n} \sigma_{ifib}.A_{ifib}.z_{ifib} \\ \sum_{ifib=1}^{n} \sigma_{ifib}.A_{ifib} \end{Bmatrix} \quad (1)$$

Where n is the number of fiber sections, x Denotes the longitudinal axis of the member, is the normal stress of i-th fiber, and is the area of i-th fiber. D(x) is resisting section force including the axial force , bending moment at section , and Refers to the fiber position in the cross section. The fibers are modeled with constitutive material models as will be discussed. The typical discrete fiber finite elements model that is used in this paper is shown in Fig. 1.

Although analysis of masonry frames by means of solid elements is the most general and versatile approach, it becomes too expensive and tedious, in the computational sense, when applied to nonlinear analysis of complex structures involving multiple members. In this case, the most common and economical

strategy is the use of nonlinear macro-elements. If a realistic nonlinear analysis of a structure can be carried out, the safety of the structure is increased and the cost can frequently be reduced (Bathe et al., 1989). An effective and more accurate approach for the modelization of the behavior of unreinforced masonry walls consists of distributing the nonlinearity along the length of the member. Therefore, to modeling the considered walls, nonlinear beam-column element is used that have distributed nonlinearity along the element and three degrees of freedom at each node included two transitive degrees of freedom and one rotational degree of freedom. Cross-section of the used beam-column element is divided into a discrete several finite regions (fibers) by a rectangular grid of lines. A schematic fiber discretization of the unreinforced masonry walls is shown in Fig. 1. The nonlinear behavior of the beam-column element at each cross section level derives entirely from the resultant nonlinear stress-strain response of the fibers. Shear effects is not included in the analyses, which is a logical estimate for medium to large span to depth ratios of the member (Spacone et al., 1996; Filippou et al., 1992). Error for the evaluation of convergences is considered to be 1e-3.

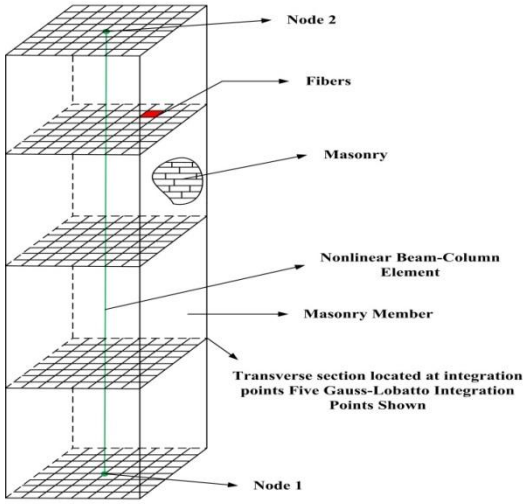

Fig. 1 Schematic of unreinforced masonry walls by fiber finite elements model

3 MATERIAL MODELING

The accuracy and reliability of the finite element analysis of unreinforced masonry walls is largely dependent on realistic material constitutive model that govern the real response of these walls. Although several models for characterizing the response of masonry material are presented in last decades, only in this paper, it is of more interest to have the simple complete model description that has a few parameters to predict accurately the constitutive behavior of masonry material. On the basic of a number of studies on constitutive model of masonry material in compression, Hognestad's model is used to define the compression behavior of masonry material. Hognestad's model included three regions: parabolic ascending stress region, linear descending region and constant residual stress region that typical curve is shown in Fig.2.

For Hognestad model, the constitutive relationship (Kaushik et al., 2007) is given in Eqs. (2-4):

$$(2) \quad \sigma_c = \left[2\left(\frac{\varepsilon}{\varepsilon_0}\right) - \left(\frac{\varepsilon}{\varepsilon_0}\right)^2 \right] \qquad \varepsilon \le \varepsilon_0$$

$$(3) \quad \sigma_c = f'_m \left[1 - 0.15\left(\frac{\varepsilon - \varepsilon_0}{\varepsilon_{cu} - \varepsilon_0}\right) \right] \qquad \varepsilon_0 \le \varepsilon \le \varepsilon_1$$

$$(4) \quad \sigma_c = 0.2 f'_m \qquad \varepsilon \ge \varepsilon_1$$

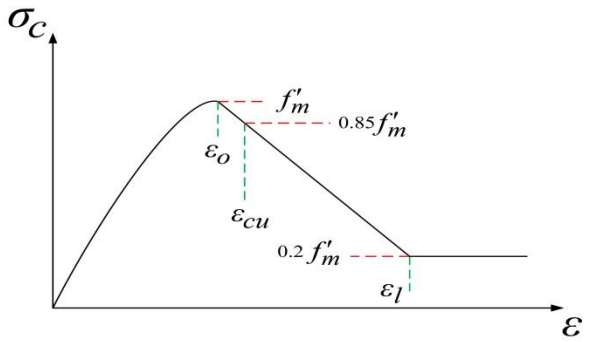

Fig. 2 Typical stress-strain curve of masonry material in compression

For tensile behavior, masonry is modeled by two constitutive stress-strain relationships. Firstly, masonry is assumed to be elastic-perfect plastic material as shown in Fig. 3.

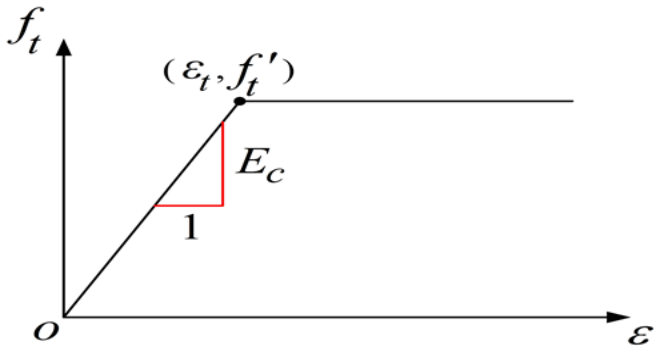

Fig. 3 Typical stress-strain curve of masonry material for elastic-perfectly plastic model in tension

For this model, the tensile stress-strain response is shown in Eqs. (5) and (6):

$$(5) \quad f_t = E_c \varepsilon \qquad \varepsilon \le \varepsilon_t$$

$$(6) \quad f_t = E_c \varepsilon_t \qquad \varepsilon \ge \varepsilon_t$$

The second model that is assumed for describe the tensile behavior of masonry comprises an ascending linear elastic portion up to the tensile strength f_t', and a descending linear portion that accounts for tension stiffening occurs after this point (Akhaveissy and Desai, 2011; Akhaveissy, 2012a). For simplicity's sake, ST (model based on softening behavior in tension) is used in the text instead of refer to the behavior

of the masonry in the second tensile model. The typical stress–strain behavior of masonry material in tension of ST is shown in Fig. 4.

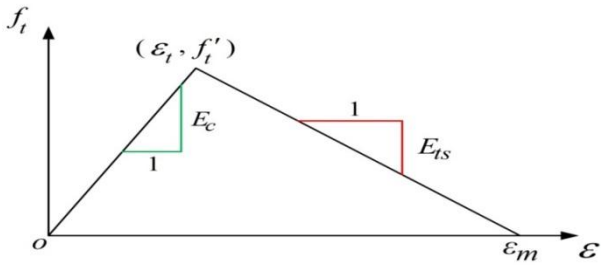

Fig. 3 Typical realistic stress-strain curve (ST model) of masonry material in tension

For ST model, the stress-strain relationship is expressed in Eqs. (7) and (8):

$$(7) \quad f_t = E_c \varepsilon \qquad \varepsilon \le \varepsilon_t$$

$$(8) \quad f_t = \lambda f_m' \left[1 - \left(\frac{\varepsilon - \varepsilon_t}{\varepsilon_m - \varepsilon_t} \right) \right] \qquad \varepsilon \ge \varepsilon_t$$

In equations (2-8), f_m' is the compressive strength of masonry prism, 0.002≤ ε_0 ≤0.004, 0.003≤ ε_{cu} ≤0.007 (Akhaveissy and Desai, 2011; Akhaveissy, 2012a), $\varepsilon_m = 10\varepsilon_t$, λ varies between 0.1 to 0.25, E_c is the modulus of elasticity of masonry, f_t' is the tensile strength of masonry, masonry tension softening stiffness $\{Ets\}$, and ε_1, ε_t are shown in Figs. 2-4.

4 PERFORMANCE LEVELS AND DRIFT CAPACITY

The response of brick masonry walls is strongly nonlinear, even at low load levels, because of the low tensile strength of the bed and head joints. As the damage due to cracking increases, masonry walls show both strength and stiffness degradation. Nowadays nonlinear static procedures are widely used for the evaluating response of structures. These procedures can be used to estimate the displacement for each level of load. The stresses and deformations in each component are evaluated at this displacement level in FEMA.

5 STRUCTURAL EXAMPLES

In this part, four structural examples are presented, namely a full scale single-story unreinforced masonry building, a two-bay two-story building, a one-bay frame and a seven-bay frame with two stories experimentally tested or analyzed by other authors which are discussed in next subsections.

In all the structural examples presented, a fiber analysis approach is used so as to predict the ultimate shear at the base for lateral loading and lateral displacement of roof. Six different material model cases are investigated in order to study the capacity curve of unreinforced masonry walls by fiber finite element

model. Each of these six cases is shown by several characters: H is presented to show the Hognestad model, the second is C explained the compression behavior, the number of 4 or 7 refers to 1000 folds of quantity , EPP is presented to exhibit the elastic-perfectly plastic material model, S is presented to explain the tension model based on softening behavior, T is shown to present the tension behavior and I is shown to explain that the maximum tensile strength of masonry in assumed tension model is changed against to experimental value. In the first case of modeling the masonry material by fiber finite element approach in this study, A Hognestad model with is utilized in order to represent the behavior of masonry in compression subsequently to modeling the tension characteristic, the elastic-perfectly plastic material is used (HC4-EPPT). Secondly, the masonry is modeled as an elastic-perfectly plastic material in tension and utilizes Hognestad model with to illustrate the compression property (HC7-EPPT). In order to study the third case, the behavior of masonry is considered as Hognestad model with in compression and the model resulted from experimental tests is assumed for tension (HC4-ST). The fourth case for predicting the masonry material behavior in compression is based on the Hognestad model with and in tension is based on the model resulted from experimental tests, respectively (HC7-ST). For the fifth case, the masonry is assumed to have a Hognestad model to represent the compression property and elastic-perfectly plastic model with idealizing the maximum of to represent the tension property (HC-EPPIT). Finally, the constitutive compression behavior is modeled using the Hognestad model and the model resulted from experimental tests with idealizing the maximum of in tension (HC-SIT). In this way, the finite element modeling and analysis approach is performed by means of the open system for earthquake engineering simulation software (OpenSees). OpenSees software framework is based on object-oriented methodologies and was developed by the pacific earthquake engineering research center at the University of California, Berkeley, which is used to simulate the structural and geotechnical systems (Mazzoni et al., 2007). To performing the nonlinear analysis, the Newton-Raphson iteration strategy is employed in the modeling. It is worth noting that, for all the cases analyzed, time analysis does not exceed from 60 seconds.

5.1 Laboratory Experiments

Initially to validate the proposed fiber finite element model, a two-story unreinforced masonry building which was tested in the form of full-scale at Pavia University is studied (Magenes and Calvi, 1997). This structure has been extensively investigated in the literature (Akhaveissy, 2012b; Belmouden and Lestuzzi, 2009; Calderini et al., 2009). The building, with a 6*4.4 m floor plan and 6.4 m in height, contains an almost independent shear wall that was in-plane loaded. The wall considered here is 250 mm thick and has two doors on the first story and two windows on second story, as shown in Fig. 5.

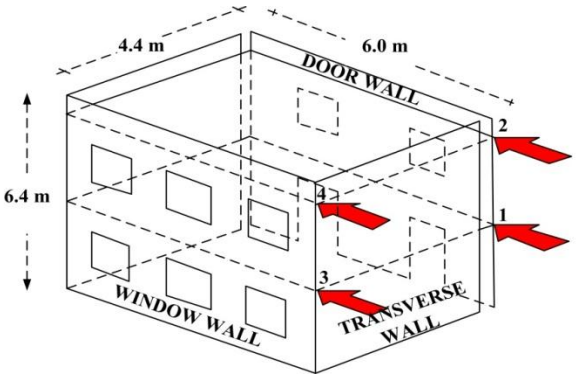

Fig. 4 Unreinforced masonry building tested at Pavia University (Belmouden and Lestuzzi, 2009)

Table 1 shows the mechanical properties of tested specimens and those parameters that are assumed in different fiber models of masonry analyzed in this example.

Table 1 Values of parameters of experimental data and different fiber models for two bay, two story masonry building

Case	Masonry model		f'_m	ε_o	ε_{cu}	f'_t	E_{ts}
	Compression	Tension					
HC4-ST	Hognestad	Softening behavior	-7.9	-0.0033	-0.004	0.07	532
HC7-ST	Hognestad	Softening behavior	-7.9	-0.0033	-0.007	0.07	532
HC4-EPPT	Hognestad	Elastic-Perfectly Plastic	-7.9	-0.0033	-0.004	0.07	0.0
HC7-EPPT	Hognestad	Elastic-Perfectly Plastic	-7.9	-0.0033	-0.007	0.07	0.0
HC-EPPIT	Hognestad	Elastic-Perfectly Plastic	-7.9	-0.0033	-0.004	0.08	0.0
HC-SIT	Hognestad	Softening behavior	-7.9	-0.0033	-0.004	0.42	532
Experimental	Hognestad	Softening behavior	-7.9	-0.0033	-	0.07	532

Note: The model based on softening behavior refers to the model that is obtained from experimental tests.

The door wall includes two exterior piers and one interior pier. The exterior pier width and axial loads on the bottom and top levels are equal to 1.15 m, 56 kN and 26.9 kN, respectively. The interior pier width and axial loads on the bottom and top levels are equal to 1.82 m, 133 kN and 64.5 kN, respectively. The loads to be applied during the pushover analysis are shown in Fig. 6.

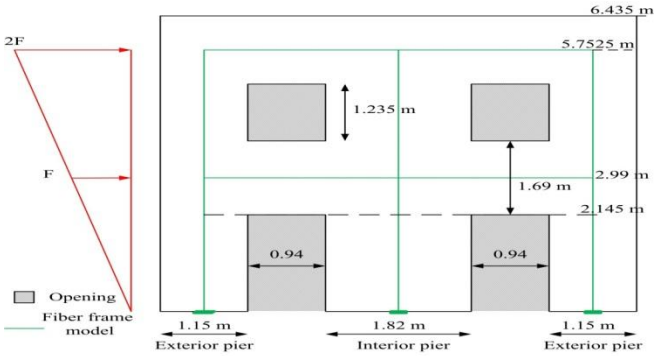

Fig. 5 Proposed fiber frame model and existing load

The pushover analysis results of fiber finite element models of a two-bay, two-story masonry frame to those obtained from experimental test are illustrated in Fig. 7.

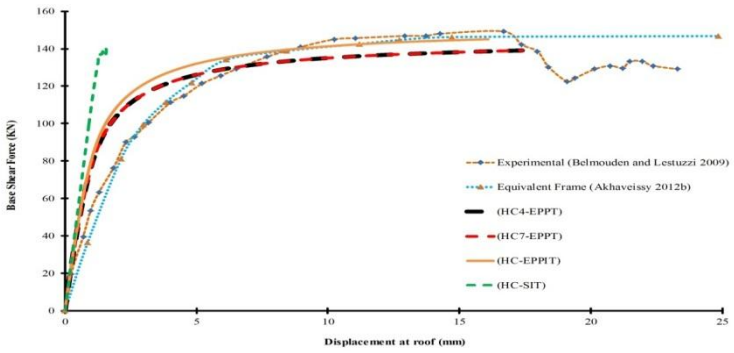

Fig. 6 Comparison from the present work and experimental test results of a two-bay, two-story masonry frame

As shown in Fig. 7, the results obtained from the models that are based on elastic perfectly plastic material model in tension show good prediction of experimental test. In this context, it can be mentioned that the pushover analysis results of fiber models disagree with test data when the real behavior of masonry material is employed in the finite element modeling. For better representation of the analyses results, the obtained results when the real behavior of masonry in tension and compression is employed are shown in Fig. 8.

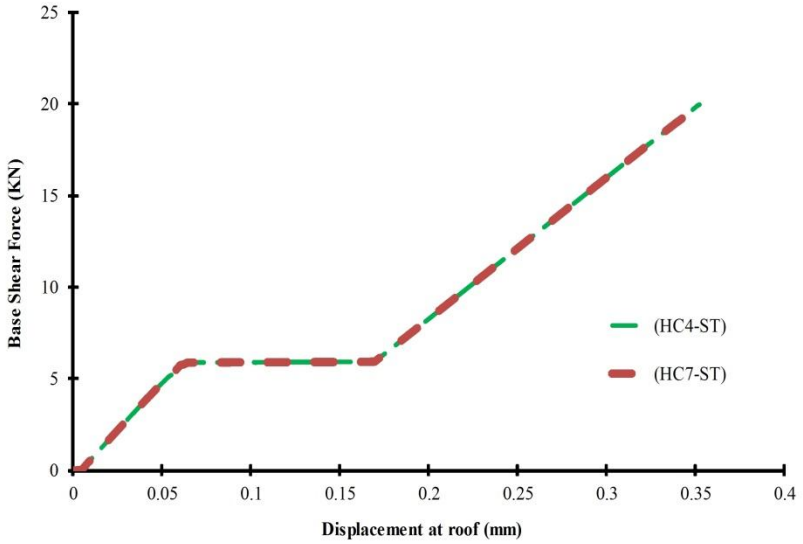

Fig. 7 Comparison detailed illustration of the results of present work modeling and experimental test

As shown in Fig. 8, the results obtained from (HC4-ST) and (HC7-ST) models are inappropriate accuracy in both maximum base shear force and maximum lateral displacement. The comparisons between different fiber model analyses results and experimental data in terms of maximum base shear force and displacement at roof is shown in Table 2.

Table 2 Comparisons of finite element analyses results and test data of two bay, two story masonry building

Results	Max. Base Shear Force	Displacement at roof
Experimental	147	23.29
HC4-EPPT	139.05	17.38
HC7-EPPT	139.05	17.38
HC4-ST	19.98	0.35
HC7-ST	19.98	0.35
HC-EPPIT	145.05	16.09
HC-SIT	140.27	1.86

As shown in Table 2, It can be mentioned that the response of the pushover analysis results disagree with test data for cases (HC4-ST), (HC7-ST) and (HC-SIT). It is illustrated that the maximum base shear force predicted for cases (HC4-ST) and (HC7-ST) is 19.98 kN. Furthermore, the value of maximum base shear force for cases (HC4-EPPT) and (HC7-EPPT) is 139.05 kN. In this point of view, the maximum lateral displacements are 17.38 mm for the cases (HC4-EPPT) and (HC7-EPPT) and 0.35 mm for the cases (HC4-ST) and (HC7-ST). Also, from the Figs. 7 and 8, it can be seen that by changing the ε_{cu} , the maximum base shear

force and corresponding maximum lateral displacement is not changed for the capacity curves of cases (HC4-EPPT) and (HC7-EPPT). Additionally, both (HC4-ST) and (HC7-ST) has the same maximum base shear force and corresponding maximum lateral displacement respectively. This conclusion means that the capacity curves is basically one curve for each both of the considered two cases that are mentioned above. The lateral displacement is predicted with relatively appropriate accuracy by cases (HC4-EPPT) and (HC7-EPPT). Additionally, in Fig. 7, it is shown that the predicted ultimate base shear force by Akhaveissy (2012b) is 147 kN whereas the experimental value was determined to be 147. Furthermore, the ultimate lateral load is estimated with relatively proper accuracy by cases (HC4-EPPT) and (HC7-EPPT). However, the tensile material model that is adopted by (HC4-EPPT) and (HC7-EPPT) is different from the real response of tensile behavior of masonry that has been obtained from experimental tests (Kaushik et al., 2007). To getting the best response of considered wall, the tensile behavior of masonry that has been obtained from experimental test is changed. For case (HC-EPPIT), the good predicted response is obtained both in maximum base shear force and corresponding lateral displacement when the maximum tensile strength is changed to 0.08 MPa. By the analysis of case (HC-EPPIT) model with this changing of value in tensile force, the maximum base shear force and corresponding lateral displacement is estimated 145.05 kN and 16.09 mm. In case (HC-SIT), the maximum base shear force is obtained when the tensile strength is 0.42 MPa, but corresponding lateral displacement is not valid. However, a Predicted result of target displacement is important role for computing the capacity curve of structures. For this case, the maximum base shear force and corresponding lateral displacement is predicted to 140.27 kN and 1.86 mm, respectively. Furthermore, to consider the damage to the structure, the acceptance criteria are evaluated in Fig. 9.

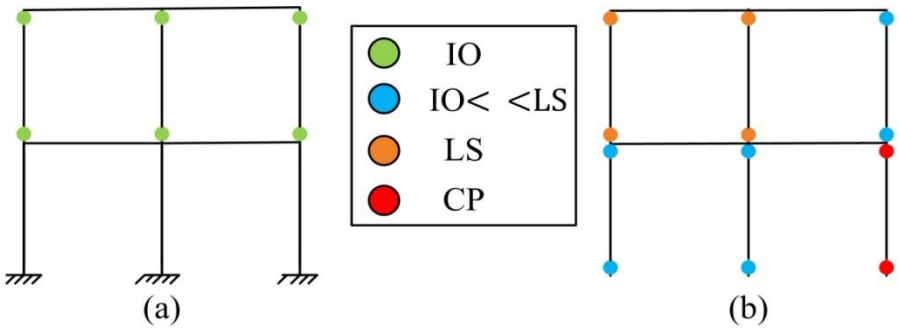

Fig. 8 Damage levels for the URM structure from the present work for case (HC-EPPIT): a) Displacement at roof equals 4.8 mm b) Displacement at roof equals 16.09 mm

Crack patterns from the experimental test of the URM building at the failure state (a top displacement equal to 24 mm) show damage to the piers for the second story and the first story as well as damage to the spandrels at the first floor. The modeling approaches considered in this research show a damage pattern incompatible with the experimental one. The predicting crack patterns displayed by the fiber finite element modeling approach of this study are different on the left lateral pier at the first level, although the numerical simulation can predict the damage level for the right pier of first story. Additionally, the damage level in the spandrels is not seen in the present work. This difference is due to the dissipation of energy by the piers. Hence, the spandrel beams behave as elastic beams (Akhaveissy, 2012b). It is worth mentioned that the experimental damage pattern is obtained from a cyclic test.

5.2 A single-story unreinforced masonry building

In this section, the fiber finite element model to simulate the capacity curve of unreinforced masonry wall is calibrated using results from a full-scale single-story unreinforced masonry building tested in the laboratory (Paquette and Bruneau, 2003, 2004, 2006). Fig. 10 illustrates the west wall of the tested model. The parapet of the west wall and the east wall was 254 mm tall (Paquette and Bruneau, 2003).

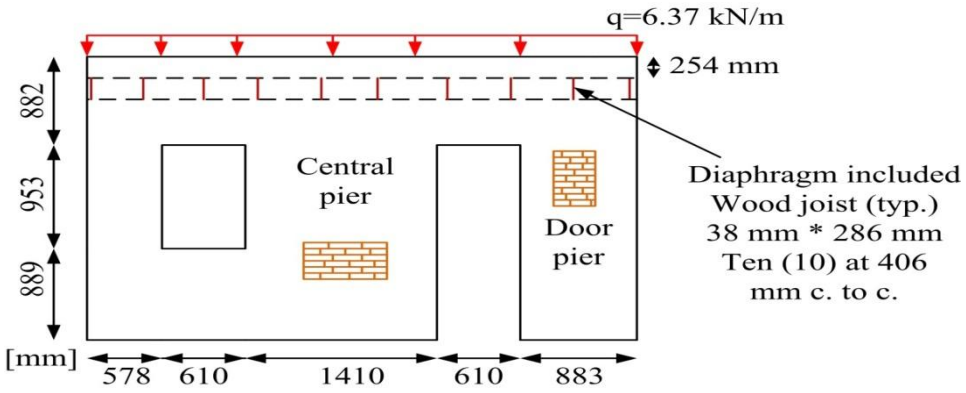

Fig. 9 Dimensions of the west wall in mm (Akhaveissy, 2012b)

The compressive strengths of the brick and mortar were 109 and 9.24 MPa, respectively, and the compressive and tensile strengths of the masonry were 22.2 and 0.18 MPa, respectively (Paquette and Bruneau, 2003). Table 3 shows the greater detailed of mechanical properties of tested specimens and those parameters that are assumed in different fiber models of masonry analyzed in this example.

Table 3 Values of parameters of experimental data and different fiber models for two bay, one story masonry building

Case	Masonry model		f'_m	ε_o	ε_{cu}	f'_t	E_{ts}
	Compression	Tension					
HC4-ST	Hognestad	Softening behavior	-22.2	-0.00235	-0.004	0.18	2100
HC7-ST	Hognestad	Softening behavior	-22.2	-0.00235	-0.007	0.18	2100
HC4-EPPT	Hognestad	Elastic-Perfectly Plastic	-22.2	-0.00235	-0.004	0.18	0.0
HC7-EPPT	Hognestad	Elastic-Perfectly Plastic	-22.2	-0.00235	-0.007	0.18	0.0
HC-EPPIT	Hognestad	Elastic-Perfectly Plastic	-22.2	-0.00235	-0.004	0.08	0.0
HC-SIT	Hognestad	Softening behavior	-22.2	-0.00235	-0.004	0.28	2100
Experimental	Hognestad	Softening behavior	-22.2	-0.00235	-	0.18	2100

Note: The model based on softening behavior refers to the model that is obtained from experimental tests.

The thickness of the wall was 190 mm. The gravity load, 2400 N/m², was applied on the diaphragm, whose dimensions were 4091 mm * 5610 mm. Ten wood joists were applied to the diaphragm in order to transmit the gravity load to the west and east walls. The net span of the wood joist was 5310 mm (Paquette and Bruneau, 2003). Therefore, the gravity load on each wall was 6.37kN/m. The west wall was also analyzed to determine the ultimate base shear force by Akhaveissy (2012b). The wall is chosen to show capability of the fiber model. The fiber model for the west wall contained 5 nonlinear beam-column

elements and 6 nodes. Fig. 11 shows the fiber frame model that is used in the analysis. The number of degrees of freedom in present work is 9 and the error for the evaluation of convergences is considered to be 1e-3.

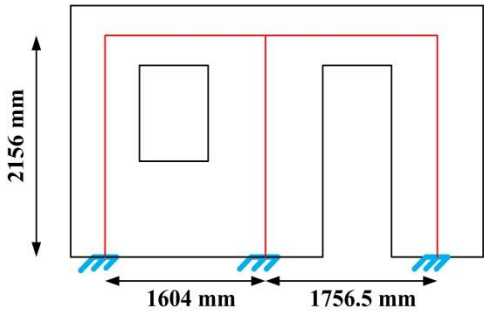

Fig. 10 Fiber frame model for the west wall

Fig. 12 illustrates the base shear force-lateral displacement response from a single-story unreinforced masonry building and results of pushover analyses of the fiber finite element models.

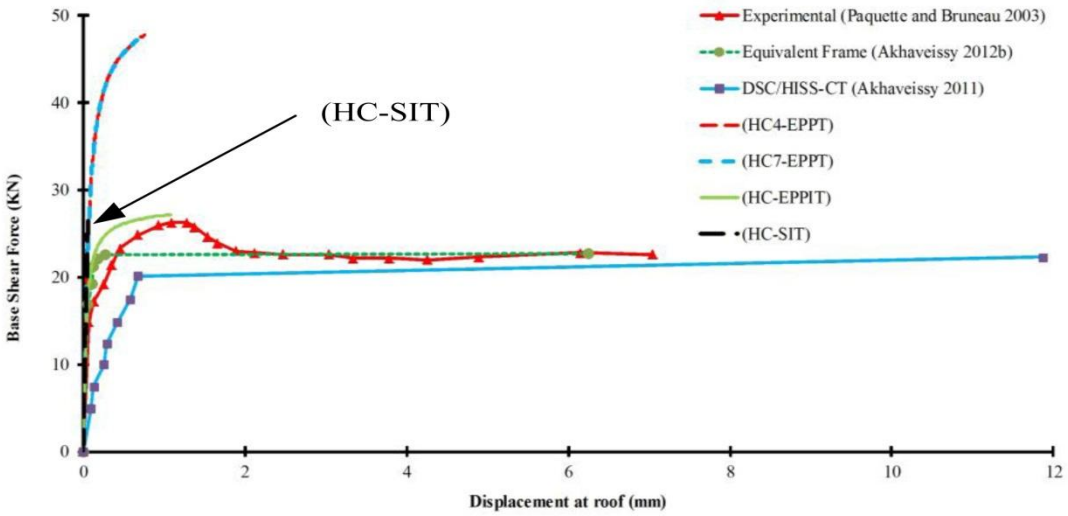

Fig. 11 Comparisons of the fiber models results and results of experimental test for two bay, one story masonry frame

As shown in Fig. 12, although the tension behavior of masonry is modeled by elastic perfectly plastic material model but the obtained results from this model when the real tensile strength of masonry is used have low accuracy against to experimental test (especially in term of maximum base shear force). Additionally, it can be mentioned that the response of the pushover analysis results disagree with test data especially in term of maximum lateral displacement when the real behavior of masonry material is employed in the finite element modeling. For better representation of the analyses results, the obtained results when the real behavior of masonry is employed in tension and compression are shown in Fig. 13.

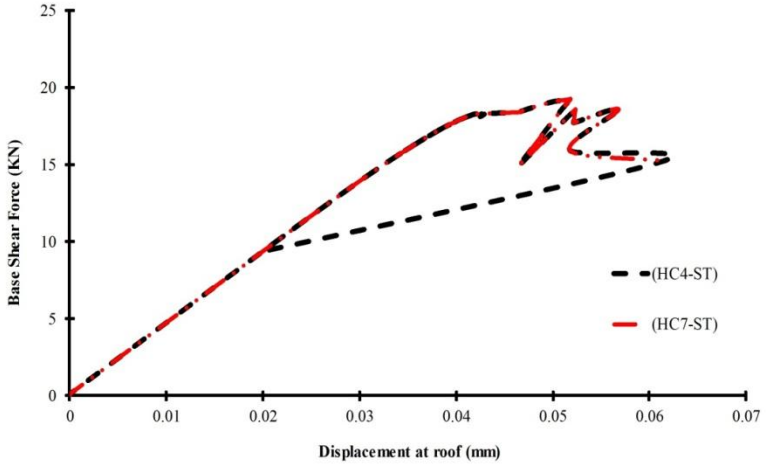

Fig. 12 Comparisons of the results for two bay, one story masonry frame of (HC4-ST) and (HC7-ST) models.

From the Figs. 12 and 13, it is demonstrated that the analyses results leads to unreasonably predictions of the behavior of URM walls when the real behavior of masonry are used. It can be observed that numerical response from the studied fiber models implemented matches the experimental results well in capturing the initial slope of the considered masonry frame. The comparisons between different fiber model analyses results and experimental data in terms of maximum base shear force and displacement at roof is shown in Table 4.

Table 4 Comparisons of finite element analyses results and test data of two bay, one story masonry building

Results	Max. Base Shear Force	Displacement at roof
Experimental	22.8	7.04
HC4-EPPT	47.7	0.75
HC7-EPPT	47.7	0.75
HC4-ST	19.25	0.06
HC7-ST	19.25	0.06
HC-EPPIT	27.21	1.08
HC-SIT	25.44	0.06

As illustrated in Table 4, the predicted maximum lateral force by cases (HC4-ST) and (HC7-ST) is 19.25 kN. However, the ultimate lateral force was obtained from experimental test to be 22.8 kN. It can be obtained that the predicted maximum base shear force for cases (HC4-EPPT) and (HC7-EPPT) is 47.7 kN. From the point of lateral displacement, it can be considered that the corresponding lateral displacement is 0.75 mm for cases (HC4-EPPT) and (HC7-EPPT). Additionally, the corresponding lateral displacement is 0.06 for (HC4-ST) and (HC7-ST). From the above results, the pushover analysis for cases (HC4-ST) and (HC7-ST) provides a relatively good prediction of the capacity curve of frame buildings in maximum base shear force but for the corresponding lateral displacement requires a correction to have better results than other proposed model. Similarly, to gaining a better result, the maximum tensile strength of masonry material is changed. The maximum base shear force is predicted 27.2 kN and 25.44 kN when is used the value of 0.08 kN and 0.28 kN for maximum tensile strength for cases (HC-EPPIT) and (HC-SIT), respectively. Moreover, the lateral displacement is estimated 1.08 mm and 0.06 mm for cases (HC-EPPIT) and (HC-SIT) respectively. It can be shown that only (HC-EPPIT) and (HC-SIT) can predict the real maximum base shear force of

experimental test. The predicted maximum base shear force by DSC/HISS-CT model (Akhaveissy and Desai, 2011) and Equivalent frame model by Akaveissy (2012) are 22.7 kN and 22.5 kN, respectively.

5.3 A one bay and seven-bay, two-story building

In addition to capability of the fiber model, two different unreinforced masonry buildings are analyzed including a one-bay frame and a seven-bay frame with two stories.

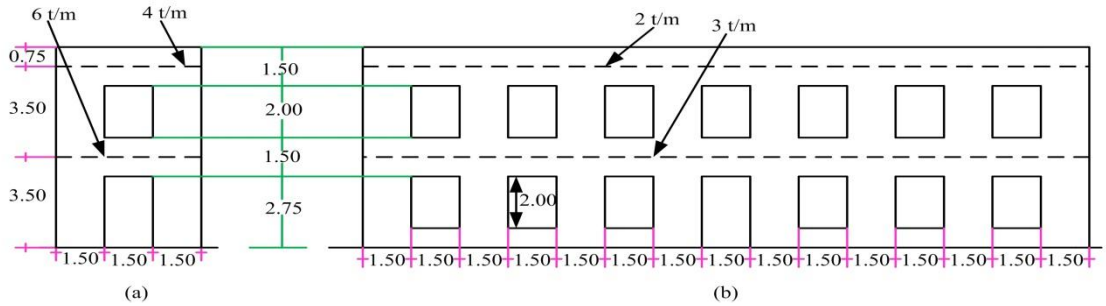

Fig. 14 (a) One-bay and (b) seven-bay two-story masonry buildings (Akhaveissy and Milani, 2013a)

These unreinforced masonry frames were analyzed by Salonikios et al. (2003). The geometrical properties of these structures are illustrated in Fig. 14. The thickness of the walls was equal to 0.6 m. The mechanical characteristics of the masonry material were as follows: the volumetric mass was $\rho = 2t/m^3$, the Young's modulus was $E_c = 1650$ MPa, the tensile strength was $f_t' = 0.1$ MPa and the compressive strength was $f_m' = 3.0$ MPa. Tables 5 and 6 show the greater detailed of mechanical properties of tested specimens and those parameters that are assumed in different fiber models of masonry analyzed in a one bay and seven-bay, two-story building.

Table 5 Values of parameters of experimental data and different fiber models for one bay, two story masonry building

Case	Masonry model		f_m'	ε_o	ε_{cu}	f_t'	E_{ts}
	Compression	Tension					
HC4-ST	Hognestad	Softening behavior	-3.0	-0.0036	-0.004	0.1	185
HC7-ST	Hognestad	Softening behavior	-3.0	-0.0036	-0.007	0.1	185
HC4-EPPT	Hognestad	Elastic-Perfectly Plastic	-3.0	-0.0036	-0.004	0.1	0.0
HC7-EPPT	Hognestad	Elastic-Perfectly Plastic	-3.0	-0.0036	-0.007	0.1	0.0
HC-EPPIT	Hognestad	Elastic-Perfectly Plastic	-3.0	-0.0036	-0.004	0.3	0.0
HC-SIT	Hognestad	Softening behavior	-3.0	-0.0036	-0.004	0.74	185
Experimental	Hognestad	Softening behavior	-3.0	-0.0036	-	0.1	185

Note: The model based on softening behavior refers to the model that is obtained from experimental tests.

Table 6 Values of parameters of experimental data and different fiber models for seven bay, two story masonry building

Case	Masonry model		f'_m	ε_o	ε_{cu}	f'_t	E_{ts}
	Compression	Tension					
HC4-ST	Hognestad	Softening behavior	-3.0	-0.0036	-0.004	0.1	185
HC7-ST	Hognestad	Softening behavior	-3.0	-0.0036	-0.007	0.1	185
HC4-EPPT	Hognestad	Elastic-Perfectly Plastic	-3.0	-0.0036	-0.004	0.1	0.0
HC7-EPPT	Hognestad	Elastic-Perfectly Plastic	-3.0	-0.0036	-0.007	0.1	0.0
HC-EPPIT	Hognestad	Elastic-Perfectly Plastic	-3.0	-0.0036	-0.004	0.3	0.0
HC-SIT	Hognestad	Softening behavior	-3.0	-0.0036	-0.004	0.85	185
Experimental	Hognestad	Softening behavior	-3.0	-0.0036	-	0.1	185

Note: The model based on softening behavior refers to the model that is obtained from experimental tests.

Details of the structures are explained as follows. In addition to the self-weight of the masonry, extra masses are considered at the floor levels. For the one-bay frame, a uniformly distributed mass of 6 tons/m was assumed for the first floor, and 4 tons/m was assumed for the second floor (Salonikios et al., 2003). The corresponding values for the seven-bay frame were assumed to be 3 and 2 tons/m, respectively (Salonikios et al., 2003).

Fig. 15 shows proposed fiber model for the one-bay and seven-bay two-story masonry frames with the lateral load pattern.

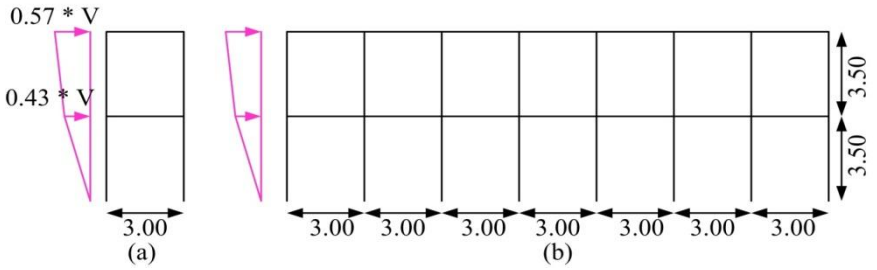

Fig. 15 Equivalent fiber frame model and lateral load pattern a) one-bay masonry building b) seven-bay masonry building

In Fig. 15, V is the value of the base shear force on the masonry frames at the failure mode. The total number of element for modeling the frame is six and thirty for one-bay building and the seven-bay frames, respectively. Hence, the numbers of degrees of freedom for the one-bay building and the seven-bay building are 12 and 48, respectively. The results of the fiber finite element analysis for a one-bay, two-story building is shown in Fig. 16.

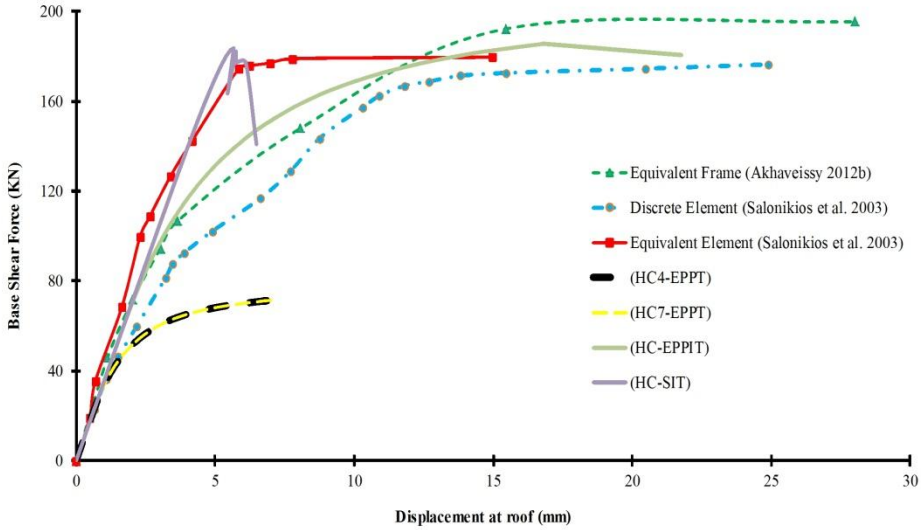

Fig. 16 Comparison the pushover curve for the one-bay, two-story masonry building

As shown in Fig. 16, the results of fiber models exhibit low prediction to those obtained from previous study. It can be mentioned that the pushover analysis results of fiber models disagree with test data in terms of maximum base shear force and maximum lateral displacement when the real behavior of masonry material is employed in the finite element modeling. For better representation of the analyses results, the obtained results when the real behavior of masonry is employed in tension and compression are shown in Fig. 17.

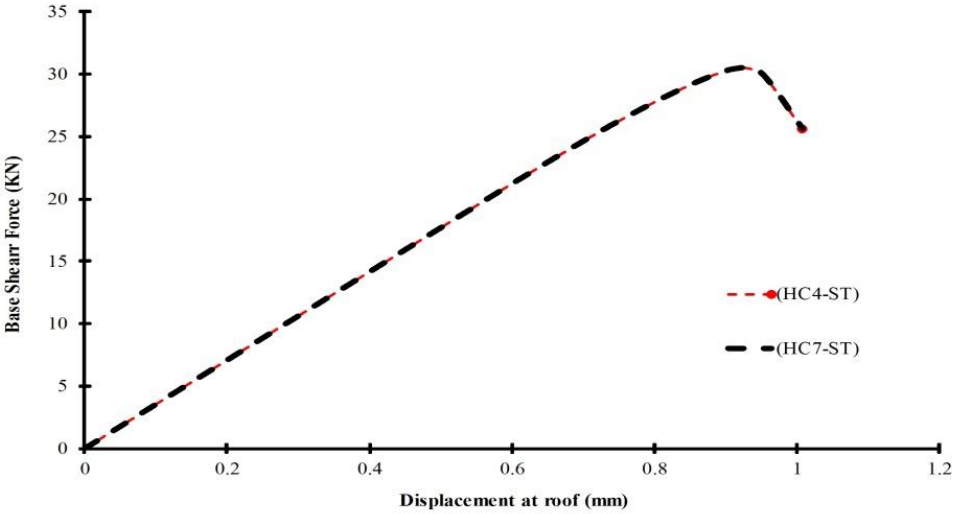

Fig. 17 The pushover curve for the one-bay, two-story masonry building

From the Figs. 16 and 17, it is shown that the estimated results are inappropriate for modeling the responses of unreinforced masonry walls when the realistic behavior of masonry in tension and compression are used. The results of the fiber finite element analysis for a seven-bay, two-story building is shown in Figs. 18 and 19.

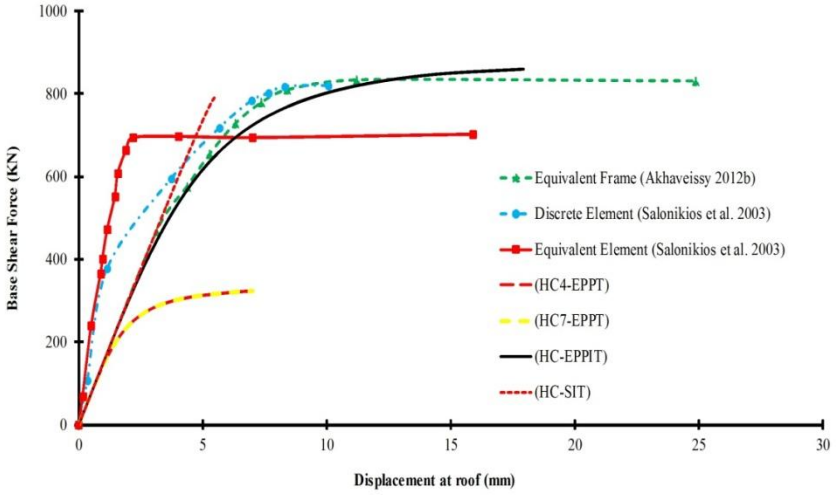

Fig. 18 Comparison the pushover curve for the seven-bay, two-story masonry building

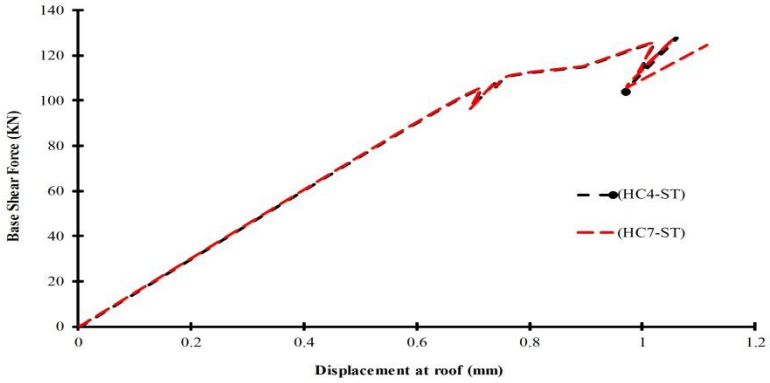

Fig. 19 The pushover curve for the seven-bay, two-story masonry building

It is illustrated (see Figs. 16-18) that the finite element response from the fiber finite element modeling by cases (HC4-EPPT), (HC7-EPPT), (HC4-ST) and (HC7-ST) approach implemented matches poor in capturing the capacity curve of considered masonry walls. For a seven-bay, two-story building, In cases (HC4-EPPT) and (HC7-EPPT) the maximum lateral displacement predicted 7.03 mm, although in cases (HC4-ST) and (HC7-ST) the maximum lateral displacement is decreased to 0.97 and 1.11 mm, respectively. Table 7 contrast differences of maximum base shear force and displacement at roof of finite element analyses results of the one-bay, two story frame.

Table 7 Comparisons of finite element analyses results and test data of one bay, two story masonry building

Results	Max. Base Shear Force	Displacement at roof
Experimental	195.55	6.86
HC4-EPPT	71.5	7.06
HC7-EPPT	71.5	7.06
HC4-ST	25.63	1.00
HC7-ST	25.63	1.00
HC-EPPIT	180.65	21.76
HC-SIT	183.7	6.48

Table 8 contrast differences of maximum base shear force and displacement at roof of finite element analyses results of the seven-bay two story frame.

Table 8 Comparisons of finite element analyses results and test data of seven bay, two story masonry building

Results	Max. Base Shear Force	Displacement at roof
Experimental	831.57	24.88
HC4-EPPT	324	7.03
HC7-EPPT	324	7.03
HC4-ST	124.6	0.97
HC7-ST	124.6	1.11
HC-EPPIT	860	17.93
HC-SIT	790	5.46

In the other hand, the values of the base shear force for the one-bay and seven-bay masonry structures predicted in the cases (HC4-EPPT) and (HC7-EPPT) are 71.5 kN and 324 kN, respectively. The maximum base shear forces when the cases (HC4-ST) and (HC7-ST) are used are estimated 25.6 kN and 124.6 kN for the one-bay and seven-bay frames. These values are 177 kN and 819 kN when using the discrete element method and 180 kN and 705 kN using the equivalent frame method as presented in the study by Salonikios et al. (2003). Accordingly, the predicted results of (HC4-EPPT), (HC7-EPPT), (HC4-ST) and (HC7-ST) are correlated unsatisfactory with the results of the previous works (Akhaveissy, 2012b; Salonikios et al., 2003).

Salonikios et al. (2003) used the equivalent frame and discrete element model in order to analyze the one-bay and seven-bay buildings. The value of the displacement at the roof of one bay frame is 15 mm and 25 mm for equivalent frame and discrete element model respectively. Furthermore, displacement at the roof in one-bay frame by Akhaveissy (2012b) model is 27.99 mm. Moreover 11.33 mm and 141.69 mm were obtained to predict displacement at the roof for seven bays frame by Akhaveissy (2012b) after step 33 and step 34 respectively. In the seven-bay frame, the maximum lateral displacement is estimated 15.8 mm and 10 mm for equivalent frame and discrete element model, respectively.

As it is discussed in two last paragraphs, the predicted results obtained from cases (HC4-EPPT), (HC7-EPPT), (HC4-ST) and (HC7-ST) is less satisfactory than results obtained from previous works (Akhaveissy, 2012b; Salonikios et al., 2003). For getting appropriate results, the maximum tensile strength of masonry material is changed. As it is shown (Figs. 16 and 18), the capacity curves obtained from analysis of case (HC-EPPIT) model have an appropriate result for one-bay and seven-bay frames when the tensile strength is changed to 0.3 kN. The maximum base shear force is estimated 180.6 kN and 860 kN for one-bay and seven-bay unreinforced masonry frames and the corresponding lateral displacement is predicted 21.76 mm and 17.93 mm. In case (HC-SIT), the maximum base shear force for one-bay and seven-bay are predicted 183.7 kN and 790 kN when tensile strength is changed to 0.74 kN and 0.85 kN, respectively. Moreover, the lateral displacement for (HC-SIT) is estimated 6.48 mm and 5.46 mm for one-bay and seven-bay frames, respectively (see Figs. 16 and 18).

6 CONCLUSIONS

This paper has presented a two-dimensional nonlinear fiber finite element models so as to predict the behavior of unreinforced masonry walls. To describe the behavior of masonry material six material models was used. To modeling the masonry material in compression Hognestad constitutive stress-strain model with different mechanical properties was used. To modeling the tensile behavior of masonry, two constitutive material models with different mechanical properties were used. Firstly, the elastic-perfectly plastic material is used. Secondly, the tensile model which is defined in two regions: linear ascending stress region up to the peak tensile stress and linear descending region that occurs after peak tensile stress was used. The main feature of the adopted constitutive masonry model was that all the parameters for showing the behavior of masonry properties can be obtained through the conventional monotonic compression and tension tests. The nonlinear beam-column element was used for modeling the considered masonry walls. Pushover analysis was performed in order to estimate the capacity curve of URM walls. The models were validated by comparing with the experimental results. It was demonstrated that the analyses results leads to unreasonably predictions of the behavior of URM walls when the real behavior of masonry material is used. Additionally, when the masonry material was modeled by elastic-perfectly plastic model in tension and Hognestad model in compression ((HC4-EPPT) and (HC7-EPPT)), the estimated results are inappropriate for modeling the responses of unreinforced masonry walls. Hence, the application of the fiber model (by using both elastic perfectly plastic material model and the model based on softening behavior in tension) are showed that the fiber finite element model employed in OpenSees cannot adequately predict the response of unreinforced masonry frames subjected to lateral loads when the real tensile strength of masonry is used. The maximum processing time of the fiber approach for the examples shown in the present paper did not exceed 60 seconds. Additionally, when the real tensile strength of masonry material was changed the finite element analyses results show appropriate predictions (especially in term of maximum base shear force) of some experimental data. In this context, although the results of these models (that are based on changing the tensile strength of masonry) in term of maximum base shear force are appropriate but these results are not reliable for researchers and engineers (because of the fragility behavior of masonry in tension that is not accounted in elastic-perfectly plastic model). Additionally, the fiber models were shown inappropriate results in comparison to experimental data in term of maximum lateral displacement; however predicted result of target displacement is important role for computing the capacity curve of structures. Furthermore, from the viewpoint of this result, it was concluded that obtained results from fiber finite element analyses employed in OpenSees are not reliable because the exact behavior of masonry material is different from the adopted masonry material models used in modeling process. An important observation is that with fiber finite element model by nonlinear beam-column element, crucial errors may be completely gained in the analysis of unreinforced masonry walls in OpenSees. Hence, the studied fiber model from OpenSees Software cannot be used to estimate the real displacements and base shear forces developed in the members due to ground motion in the unreinforced masonry structures. Furthermore, for the future researches and practical engineering projects, it is proposed to use equivalent frame model that has been presented by Akhaveissy (2012b).

References

Adeli, M. M., Deylami, A., Banazadeh, M., & Alinia, M. M. (2011). A Bayesian approach to construction of probabilistic seismic demand models for steel moment-resisting frames. *Scientia Iranica Transactions A: Civil Engineering*, 18, 885-894.

Akhaveissy, A. H. (2011). Lateral strength force of URM structures based on a constitutive model for interface element. *Latin American Journal of Solids and Structures*, 8, 445-461.

Akhaveissy, A. H., & Desai, C. S. (2011). Unreinforced masonry walls: nonlinear finite element analysis with a unified constitutive model. *Archives of Computational Methods in Engineering*, 18, 485-502.

Akhaveissy, A. H. (2012a). The DSC model for the nonlinear analysis of in-plane loaded masonry structures. *The Open Civil Engineering Journal*, 6, 200-214.

Akhaveissy, A. H. (2012b). Finite element nonlinear analysis of high-rise unreinforced masonry building. *Latin American Journal of Solids and Structures*, 9, 547-567.

Akhaveissy, A. H. (2013). Limit state strength of unreinforced masonry structures. *Earthquake Spectra*, 29, 1-31.

Akhaveissy, A. H., & Milani, G. (2013a). Pushover analysis of large scale unreinforced masonry structures by means of a fully 2D non-linear model. *Construction and Building Materials*, 41, 276–295.

Akhaveissy, A. H., & Milani, G. (2013b). A numerical model for the analysis of masonry walls in-plane loaded and strengthened with steel bars. *International Journal of Mechanical Sciences*, 72, 13-27.

Akhaveissy, A. H., Ghahfarokhi, M. R., & Zahraie, M. (2013). An efficient algorithm for modelling nonlinear behavior of reinforced concrete beams using macro elements. *Journal of Computational Methods in Engineering*, 31, 61-78. (In Persian)

Aschheim, M., Tjhin, T., Comartin, C., Hamburger, R., & Inel, M. (2007). The scaled nonlinear dynamic procedure. *Engineering Structures*, 29, 1422-1441.

Asgarian, B., Sadrinezhad, A., & Alanjari, P. (2010). Seismic performance evaluation of steel moment resisting frames through incremental dynamic analysis. *Journal of Constructional Steel Research*, 66, 178-190.

Bathe, K. J., & Cimento, A. P. (1980). Some practical procedure for the solution of nonlinear finite element equations. *Computer Methods in Applied Mechanics and Engineering*, 22, 59-85.

Bathe, K. J., Walczak, J., Welch, A., & Mistry, N. (1989). Nonlinear analysis of concrete structures. *Computers and Structures*, 32, 563-590.

Belmouden, Y., & Lestuzzi, P. (2009). An equivalent frame model for seismic analysis of masonry and reinforced concrete buildings. *Construction and Building Materials*, 23, 40-53.

Bruneau, M. (1995). Performance of masonry structures during the 1994 Northridge (Los Angeles) Earthquake. *Canadian Journal of Civil Engineering*, 22, 378-402.

Calderini, C., Cattari, S., & Lagomarsino, S. (2009). In plane seismic response of unreinforced masonry walls: comparison between detailed and equivalent frame models, *ECCOMAS Thematic Conference on Computational Methods in Structural Dynamics and Earthquake Engineering, Rhodes, Grecce, June.*

Cecchi, A., & Milani, G. (2008). A kinematic FE limit analysis model for thick English bond masonry walls. *International Journal of Solids and Structures*, 45, 1302-1331.

FEMA-307 (1999). Evaluation of earthquake damaged concrete and masonry wall buildings, *Federal Emergency Management Agency, Washington (DC), USA.*

Filippou, F. C., D'Ambrisi, D., & Issa, A. (1992). Nonlinear static and dynamic analysis of reinforced concrete subassemblages, *EERC Report 92/08, Earthquake Engineering Research Center, University of California, Berkeley (USA).*

Hamutcuoglu, O. M., & Scott, M. H. (2009). Finite element reliability analysis of bridge girders considering moment–shear interaction. *Structural Safety*, 31, 356–362.

Hashemi, S. S., & Vaghefi, M. (2011). Cyclic analysis of RC frames with respect to employing different methods in the fiber model for consideration of bond-slip effect. *Turkish Journal of Engineering and Environmental Science*, 35, 1-18.

Jiang, Y., Li, G., & Yang, D. (2010). A modified approach of energy balance concept based multimode pushover analysis to estimate seismic demands for buildings. *Engineering Structures*, 32, 1272-1283.

Jingjiang, S., Ono, T., Yangang, Z., & Wei, W. (2003). Lateral load pattern in pushover analysis. *Earthquake Engineering and Engineering Vibration*, 2, 99-107.

Kaushik, H. B., Rai, D. C., & Jain, S. K. (2007). Stress-strain characteristics of clay brick masonry under uniaxial compression. *Journal of Material in Civil Engineering ASCE*, 19, 728–739.

Lee, T. H., & Mosalam, K. M. (2004). Probabilistic fiber element modeling of reinforced concrete structures. *Computers and Structures*, 82, 2285–2299.

Magenes, G., & Calvi, G. M. (1997). In-plane seismic response of brick masonry walls. *Earthquake Engineering and Structural Dynamics*. 26, 1091-1112.

Makarios, T. K. (2005). Optimum definition of equivalent non-linear SDF system in pushover procedure of multistory r/c frames. *Engineering Structures*, 27, 814–825.

Mazzoni, S., Mckenna, F., Scott, M. H., & Fenves, G. L. (2007). OpenSees command language manual, *Pacific Earthquake Engineering Research Center, University of California, Berkeley (USA)*, (http://opensees.berkeley.edu/).

Melo, J., Fernandes, C., Varum, H., Rodrigues, H., Costa, A., & Arêde, A. (2011). Numerical modelling of the cyclic behaviour of RC elements built with plain reinforcing bars. *Engineering Structures*, 33, 273-286.

Milani, G., Lourenco, P. B., & Tralli, A. (2006). Homogenised limit analysis of masonry walls *Part I: Failure surfaces. Computers and Structures*, 84, 166-180.

Milani, G., Lourenco, P. B., & Tralli, A. (2007). 3D homogenized limit analysis of masonry buildings under horizontal loads. *Engineering Structures*, 29, 3134-3148.

Milani, G. (2011). Simple homogenization model for the non-linear analysis of in-plane loaded masonry walls. *Computers and Structures*, 89, 1586-1601.

Milani, G., Sanjust, C. A., Casolo, S., & Taliercio, A. (2012). Maniace castle in Syracuse, Italy: Comparison between present structural situation and hypothetical original configuration by means of full 3D FE models. *The Open Civil Engineering Journal*, 6, 173-187.

Moghaddam, H. A. (2006). *Seismic design of masonry building, Sharif University Press, Tehran, Iran. (In Persian)*

Paquette, J., & Bruneau, M. (2003). Pseudo- dynamic testing of unreinforced masonry building with flexible diaphragm. *Journal of Structural Engineering ASCE*, 129, 708-716.

Paquette, J., & Bruneau, M. (2004). Pseudo- dynamic testing of unreinforced masonry building with flexible diaphragm, *13th World Conference on Earthquake Engineering, Vancouver, Canada, August*.

Paquette, J., & Bruneau, M. (2006). Pseudo- dynamic testing of unreinforced masonry building with flexible diaphragm and comparison with existing procedures. *Construction and Building Materials*, 20, 220-228.

Park, J., Towashiraporn, P., Craig, J. I., & Goodno, B. J. (2009). Seismic fragility analysis of low-rise unreinforced masonry structures. *Engineering Structures*, 31, 125-137.

Pasticier, L., Amadio, C., & Fragiacomo, M. (2008). Non-linear seismic analysis and vulnerability evaluation of a masonry building by means of the sap2000 v.10 code. *Earthquake Engineering and Structural Dynamics*, 37, 467-485.

Roca, P., Cervera, M., Pelà, L., Clemente, R., & Chiumenti, M. (2012). Viscoelasticity and damage model for creep behavior of historical masonry structures. *The Open Civil Engineering Journal*, 6, 188-199.

Rodrigues, H., Varum, H., & Costa, A. G. (2012). A simplified shear model for reinforced concrete elements subjected to reverse lateral loadings. *Central European Journal of Engineering*, 2, 136-145.

Rota, M., Penna, A., & Magenes, G. (2010). A methodology for deriving analytical fragility curves for masonry buildings based on stochastic nonlinear analyses. *Engineering Structures*, 32, 1312-1323.

Salonikios, T., Karakostas, C., Lekidis, V., & Anthoine, A. (2003). Comparative inelastic pushover analysis of masonry frames. *Engineering Structures*, 25, 1515-1523.

Shamsaia, M., Sezena, H., & Khaloob, A. (2007). Behavior of reinforced concrete beams post-tensioned in the critical shear region. *Engineering Structures*, 29, 1465–1474.

Shao, Y., Aval, S., & Mirmiran, A. (2005). Fiber-element model for cyclic analysis of concrete-filled fiber reinforced polymer tubes. *Journal of Structural Engineering ASCE*, 131, 292–303.

Spacone, E., Filippou, F. C., & Taucer, E. F. (1996). Fiber beam-column model for non-linear analysis of RC frames: Part I. formulation. *Earthquake Engineering and Structural Dynamics*, 25, 711-725.

Taucer, F. F., Spacone, E., & Filippou, F. C. (1991). A fiber beam-column element for seismic response analysis of reinforced concrete structures, *EERC Report 91/17, Earthquake Engineering Research Center, University of California, Berkeley (USA).*